

Supplementary data

Enhanced photocatalytic activity of TiO₂/UiO-67 under visible-light for Aflatoxin B1 degradation

Jia Zhang ^a, Xintong Gao ^b, Wenbo Guo ^b, Zengnan Wu ^b, Yilin Yin ^b and Zenghe Li ^{*a}

College of Chemistry, Beijing University of Chemical Technology, Beijing, 100029, PR China.

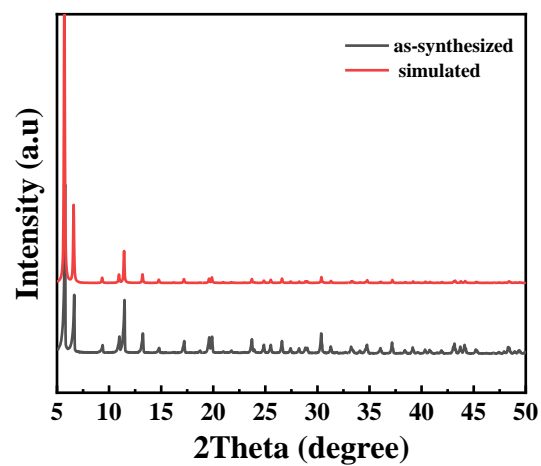


Fig. S1 XRD patterns for synthesized UiO-67, simulated pattern from crystal structure data.

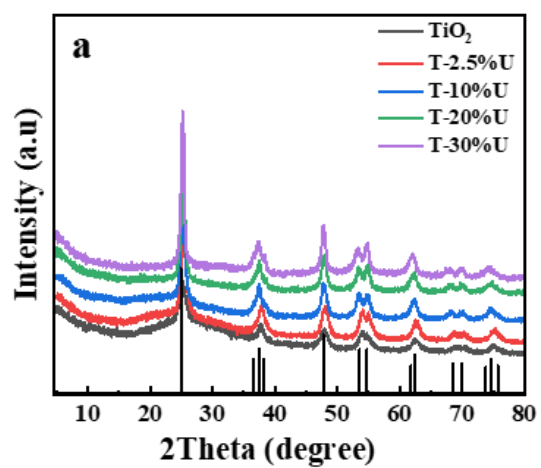


Fig. S2 XRD patterns for (a) T-XU nanoparticles (X= 2.5%, 10%, 20%, 30%), synthesized TiO₂ and simulated pattern for TiO₂.

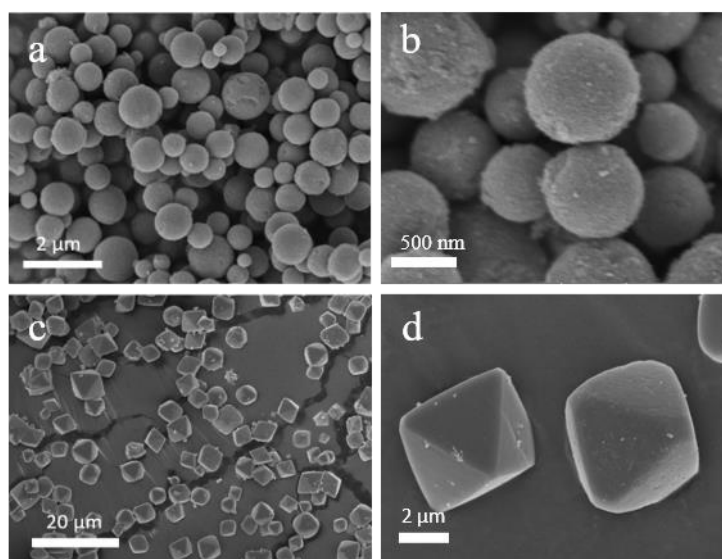


Fig. S3 SEM images of (a-b) TiO₂ nanoparticles and (c-d) UiO-67 at different magnifications.

The XRD pattern of the as-synthesised UiO-67 was shown in Fig. S1, and the peaks appeared at the 2θ of 5.6° , 6.5° , 11.2° , and 17.2° are entirely consistent with the typical crystal structure of UiO-67, suggesting the successful synthesis of pure UiO-67. In addition, the crystal morphology of UiO-67 and TiO₂ was characterized by SEM. TiO₂ nanospheres exhibit perfect sphere morphology and smooth surface and particle size range from 0.5 to 1 μm . The octahedral nanocrystals of UiO-67 are clearly displayed, and individual microcrystals with edge lengths are around 2 - 5 μm in Fig. S3 (c-d). Interestingly, with the doping of UiO-67, the morphology of TiO₂ transferred from nanospheres.

In this study, all vessels contaminated by AFB1 should be soaked in sodium hypochlorite solution (2% w/v) for 24 h and then washed with ethanol.

The experiment of XRD patterns taken from $2\theta = 5^\circ$ onwards instead of 20° was added, and the result is shown in Fig. S2. However, no obvious peaks of UiO-67 were observed in pattern of the T-XU, including T-30%U (30% was the mass ratio of UiO-67 with respect to the tetrabutyl titanate). The result of XRD indicated that the T-XU composites were mainly composed by TiO₂ and negligible doping amount of UiO-67.

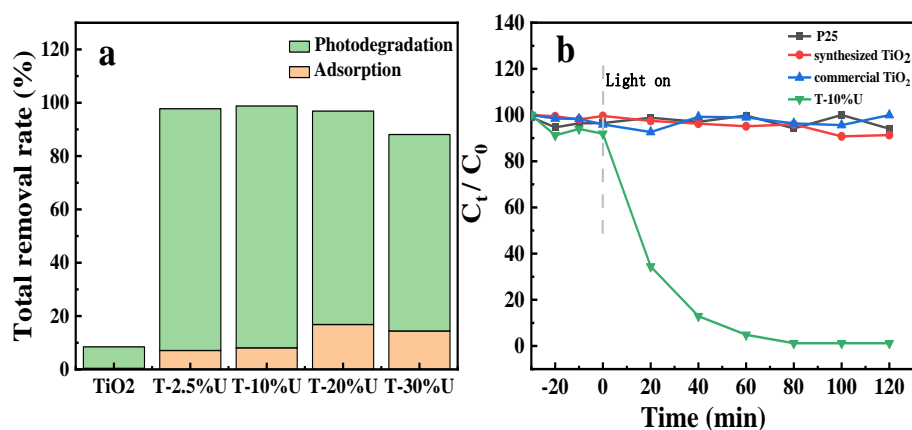


Fig. S4 (a) Total removal rate of TiO₂, T-XU. (b) Photocatalytic degradation of AFB1 over T-10%U, commercial TiO₂, synthesized TiO₂, the commercial P25 under visible light irradiation.

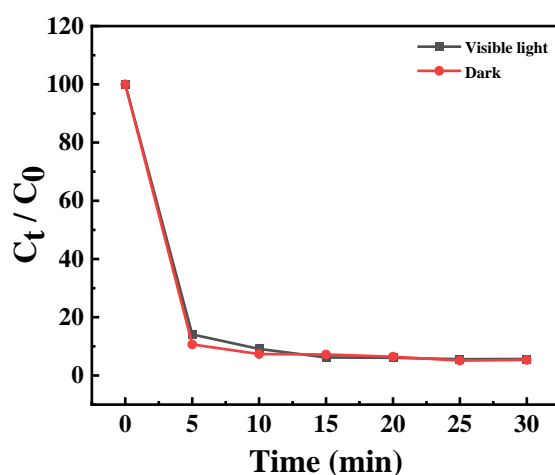


Fig. S5 photodegradation of AFB1 over UiO-67 with/without visible light.

Table. S1 Photodegradation rate of AFB1 over UiO-67 with/without visible light.

	5 min	10 min	15 min	20 min	25 min	30 min
Dark	85.90%	90.87%	93.8%	93.93%	94.38%	94.33%
Visible light	89.32%	92.63%	92.79%	93.57%	94.89%	94.64%

As shown in Fig. S5 and Table S1, the photodegradation rate of UiO-67 is similar to the adsorption percentages in dark condition. After 30 min, the removal rate of AFB1 in dark conditions reached 94.33%, while the photodegradation rate just reached 94.67%. Thus, we concluded that UiO-67 has high adsorption efficiency and poor photodegradation efficiency under visible light.

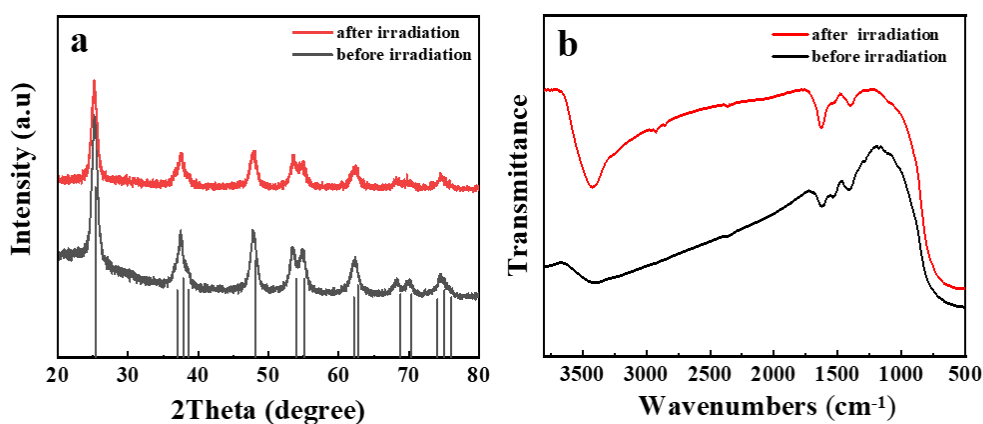


Fig. S6 (a) XRD patterns and (b) FT-IR spectra of T-10%U before and after irradiation for 4 cycle reaction.

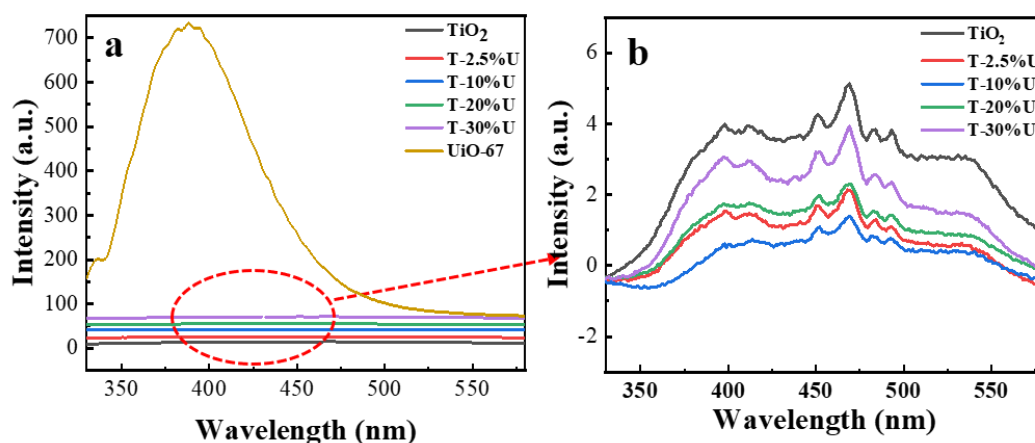


Fig. S7 (a) PL spectra of T-XU nanoparticles, TiO₂ and UiO-67. (b) PL spectra of T-XU nanoparticles and TiO₂.

The PL spectra of UiO-67 have been added. As shown in Fig. S7, UiO-67 possessed high fluorescent intensity compared with T-XU and TiO₂. In fact, UiO-67 is a fluorescent MOF according to a previous report,¹ while traditional semiconductors have low fluorescence intensity. PL spectra were usually used to evaluate the recombination rate of traditional semiconductors photocarriers. Therefore, The PL spectra of UiO-67 have been added in supporting information.

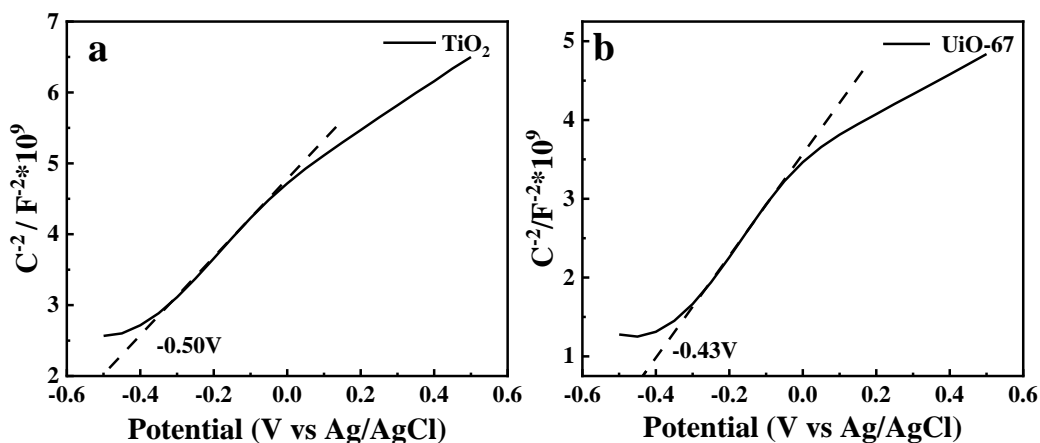


Fig. S8 Mott-Schottky plots for TiO₂ (a) and UiO-67 (b).

Table. S2 Pseudo 1st order model parameters for the degradation of AFB1 onto T-XU composites.

	T-2.5%U	T-10%U	T-20%U	T-30%U
k/min ⁻¹	0.02808	0.05306	0.02799	0.01625
t _{1/2} (min)	24.68	13.06	24.76	42.66
线性回归系数 R ²	0.9626	0.9922	0.9927	0.9953

Table. S3 Comparison of AFB1 photodegradation of various reported photocatalysts.

Catalyst	Light source	The amount of catalyst (mg)	AFB ₁ concentration (ppm)	Photocatalysis Degradation time/rate (%)	Reference
Nanosized g-C ₃ N ₄ sheets	500 W Xenon lamp (λ>400 nm)	10 mg	100 mL 0.5 ppm	120 min 70.2%	2
WO ₃ /RGO/g-C ₃ N ₄ composite	300 W Xenon lamp (λ>420 nm)	10 mg	100 mL 0.54 ppm	120 min 92%	3
Clew-like WO ₃ Decorated with CdS	300 W Xenon lamp (λ>420 nm)	10 mg	100 mL 0.46 ppm	80 min 95.5%	4
T-10%U	300 W Xenon lamp (λ>420 nm)	10 mg	100 mL 0.5 ppm	80 min 98.8%	This report

References

1. Y. Han, X. He, W. Yang, X. Luo, Y. Yu, W. Tang, T. Yue and Z. Li, *Food Chem.*, 2021, **345**, 128839.
2. J. Mao, L. Zhang, H. Wang, Q. Zhang, W. Zhang and P. Li, *Chemical Engineering Journal*, 2018, **342**, 30-40.
3. J. Mao, Q. Zhang, P. Li, L. Zhang and W. Zhang, *Chemical Engineering Journal*, 2018, **334**, 2568-2578.
4. J. Mao, P. Li, J. Wang, H. Wang, Q. Zhang, L. Zhang, H. Li, W. Zhang and T. Peng, *Applied Catalysis B: Environmental*, 2019, **248**, 477-486.